Of Mice and Men: Increased dendritic complexity gives rise to unique human networks

Lida Kanari*[1], Ying Shi[1], Alexis Arnaudon[1] Natali Barros Zulaica[1], Ruth Benavides-Piccione[2], Jay S. Coggan[1], Javier DeFelipe[2], Kathryn Hess[3], Huib D. Mansvelder[4], Eline J. Mertens[4], Idan Segev[5], Henry Markram[1] and Christiaan P.J. de Kock[4]

[1]Blue Brain Project, Ècole Polytechnique Fèdèrale de Lausanne (EPFL), Campus Biotech, 1202 Geneva, Switzerland.
[2]Laboratorio Cajal de Circuitos Corticales, Universidad Politècnica de Madrid and Instituto Cajal (CSIC), Pozuelo de Alarcòn, Madrid 28223, Spain
[3]Laboratory for Topology and Neuroscience, Brain Mind Institute, Ècole Polytechnique Fèdèrale de Lausanne (EPFL), 1015 Lausanne, Switzerland
[4]Department of Integrative Neurophysiology, Center for Neurogenomics and Cognitive Research, Vrije Universiteit Amsterdam, 1081 HV Amsterdam, the Netherlands
[5] Department of Neurobiology and Edmond and Lily Safra Center for Brain Sciences, The Hebrew University of Jerusalem, 9190501 Jerusalem, Israel
* Corresponding author: lida.kanari@gmail.com

September 11, 2023

Abstract: The organizational principles that distinguish the human brain from those of other species have been a long-standing enigma in neuroscience. Here, we leverage advances in algebraic topology to uncover the structural properties of the human brain at subcellular resolution. First, we reveal a much higher perisomatic branching density in pyramidal neurons when comparing homologous cortical regions in humans and mice. Traditional scaling methods consistently fail to interpret this difference, suggesting a distinctive feature of human pyramidal neurons. We next show that topological complexity leads to highly interconnected pyramidal-to-pyramidal and higher-order networks, which is unexpected in view of reduced neuronal density in humans compared to mouse neocortex. We thus present robust evidence that reduced neuronal density but increased topological complexity in human neurons ultimately leads to highly interconnected cortical networks. The dendritic complexity, which is a defining attribute of human brain networks, may serve as the foundation of enhanced computational capacity and cognitive flexibility.

Keywords: Human; Rodent; Neuron morphology; Topological analysis; Morphological comparison; Pyramidal cell

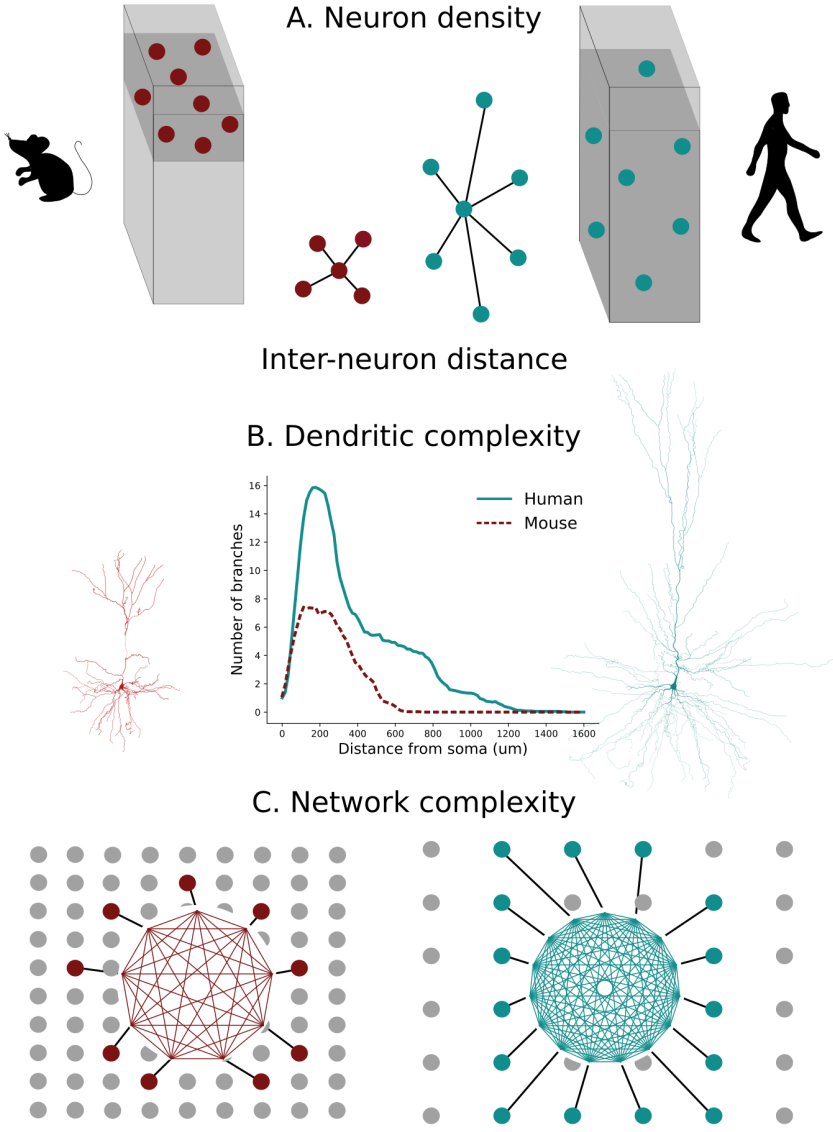

Graphical abstract. A. Human neural networks are different from mice due to their lower neuron density, resulting in increased distances between neurons, particularly among pyramidal cells. B. The topological analysis of layer 2/3 pyramidal cells in the cortex reveals an intriguing difference: human neurons exhibit a significantly larger number of dendritic branches, especially near the cell body compared to mice. This phenomenon is termed "higher topological complexity" in dendrites. C. The combination of reduced neuron density and enhanced dendritic complexity results in greater network complexity within the human brain. Network complexity is defined by larger groups of neurons forming complex interconnections throughout the network. Our findings suggest that dendritic complexity wields a more substantial influence on network complexity than neuron density does, hinting at a potential strategy for enhancing cognitive abilities.

Introduction

The question of how the brain contributes to human cognition has been a topic of debate and discussion since ancient times. The shift from Aristotle's belief that intellect resided in the heart to Gallen's assertion of the brain's significance in ancient Rome marked a pivotal moment in this ongoing discourse. Humans have long been intrigued by the reasons behind their own relative sophistication compared to other animals (Cairò, 2011), sparking deep curiosity about the unique capabilities of the human brain. Initially, it was postulated that human cognitive prowess was linked to the sheer magnitude of our brains (Cairò, 2011), stemming from the notion that intelligence is directly correlated with brain size. However, research has failed to identify similar abilities in other large-brained animals, such as elephants (Hart et al., 2001) and cetaceans (Waugh and Thewissen, 2021). Furthermore, subsequent studies (Hofman, 1988) systematically analyzing the ratio of brain to body mass refuted these theories, demonstrating that human brain size is not distinctive compared to other animals. Nevertheless, the conviction that the human brain is exceptional among mammalian brains persists, as indicated by the numerous studies that investigate possible correlations of human intelligence with larger cell counts (Herculano-Houzel, 2009), cortical thickness (Menary et al., 2013; Hopkins et al., 2019), increased cortical folding (Gregory et al., 2016) or dendritic size (Galakhova et al., 2022). However, despite extensive endeavors to unravel its mysteries, numerous aspects of our unique characteristics remain elusive. While there may well be other factors at play in defining human intelligence, in this study we demonstrate that the shapes of dendrites are an important indicator of network complexity that cannot be disregarded in our quest to identify what makes us human.

Ramon y Cajal sparked the intriguing question of the possible presence of distinctive structural characteristics in human neurons that contribute to their optimal functioning when compared to neurons in other species. Numerous studies have examined the unique functional, molecular, and structural features of human neurons (DeFelipe et al., 2002). However, it's only recently that significant progress has been made in addressing the knowledge gap concerning distinctive features of human neurons by integrating multimodal datasets that encompass single neuron morphologies, neurochemistry, electrophysiology, and transcriptomics (Beaulieu-Laroche et al., 2021; Berg et al., 2021; Bakken et al., 2021; Kalmbach et al., 2021). Several laboratories (Mohan et al., 2015; Deitcher et al., 2017; Benavides-Piccione et al., 2019; Berg et al., 2021) have contributed valuable insights into the structural properties of human neurons by generating morphological reconstructions. In parallel, detailed electron microscopy (EM) reconstructions of human brain tissue (Rollenhagen et al., 2020; Cano-Astorga et al., 2021; Loomba et al., 2022; Cano-Astorga et al., 2023) have provided important information regarding the composition and connectivity properties of human neurons. These recent advancements in data generation are enabling a more comprehensive exploration of the intricate structural properties of human neurons and their potential implications for neural function.

In this study, we leveraged these invaluable resources to create a large collection of neurons, normalized with respect to orthogonal factors, such as age, brain region and cortical thickness. Our primary focus was the comparative analysis of human and mouse pyramidal cells, specifically within layer 2/3 of the human association temporal cortex (which is homologous to the temporal association cortex in mice). Through a meticulous morphological investigation, we corroborated previous findings (Mohan et al., 2015; Benavides-Piccione et al., 2019) indicating that human neurons exhibit greater total length and extend further from the soma. Additionally, our topological analysis (Kanari et al., 2018) unveiled a distinctive pattern of high branching density surrounding the soma in human neurons, a trait absent in the mouse cortical dendrites. These results were found to be consistent across other cortical layers (e.g., layer 5) and brain regions (e.g., hippocampus), implying that this topological difference may be a universal feature distinguishing human neuron morphologies from those of rodents.

Having established that size scaling, whether uniform or not, fails to adequately account for the observed topological differences, we embarked on a thorough investigation to unravel the underlying factors and discern the potential functional significance of these fundamental distinctions between species in these cortical areas. An assiduous analysis of the anatomical properties of the cortex, based on dense tissue reconstructions (Loomba et al., 2022) and detailed anatomical studies (DeFelipe et al., 2002; Benavides-Piccione et al., 2002) indicated a significantly lower cell density in the human cortex, leading to greater inter-neuron distances, with the average closest neighbor distance between human neurons being almost twice that in the mouse. This distinctive property proved pivotal in elucidating the observed topological disparities.

In order to maintain dendritic density within the cortical tissue, despite the greater inter-neuronal distances, individual neurons must possess greater dendritic length. This hypothesis was initially proposed based on old histological studies (by Franz Nissl and Constantin Von Economo), suggesting that the wider separation of neurons in humans, compared to other species, could indicate a higher level of refinement in the connections between neurons (DeFelipe, 2011). However, a direct correlation between neuronal density and dendritic complexity was not established at that time. In our current study, we demonstrate this direct relation between neuron density and dendritic length. Moreover, the distribution of additional dendritic branches in close proximity to the soma confers the advantageous ability to fill the inter-neuronal space, while preserving the connection probability between neurons. Furthermore, our investigation revealed that the combination of lower neuronal density and greater dendritic complexity resulted in a considerable increase in the number of simplices (Sizemore et al., 2016; Reimann et al., 2017) within human networks, suggesting the presence of abundant, strongly connected sub-networks within the human cerebral cortex.

The findings of our study suggest that a fundamental geometric principle underlies the observed variations in neuronal characteristics, which in turn has significant implications for the structural organization of human networks. Specifically, human networks exhibit a

preference for greater complexity of individual cells, as opposed to the greater neuron density observed in mouse networks. This seemingly straightforward yet powerful distinction raises an intriguing question: does the augmentation of complexity within network nodes (i.e. dendrites) confer a cognitive advantage compared to increasing the number of nodes (i.e. neurons)? While the necessary data to fully answer this question are not readily available, it is reasonable to speculate that the combination of highly complex dendrites and strongly connected networks contributes to the high capacity for information processing of the human brain. These findings shed light on mechanisms possibly underlying the exceptional cognitive abilities exhibited by humans and highlight the significance of considering the interplay between neuronal complexity and network organization in understanding brain function.

Results

Human cortex has lower neuronal density and larger inter-neuron distances

Contrary to previous assumptions, the size of the brain is not a proxy for the number of neurons it contains (Herculano-Houzel, 2009). In particular, despite the increase in cell counts observed in the human brain (DeFelipe et al., 2002), the lower neuron density in the human cortex ($\approx 25700/mm^3$) compared to the mouse cortex ($\approx 137600/mm^3$) challenges this notion. Another important difference is the significantly higher proportion of interneurons, comprising 30% of human neurons compared to a mere 12% in the mouse (DeFelipe, 2011; Loomba et al., 2022).

In order to investigate the effect of lower neuron density on the spatial distribution of neurons, we computed the distance between the cells, assuming a uniform distribution of neurons within a cortical layer. The closest neighbor distance between human neurons is $\approx 19\mu m$, which is nearly twice that of mice at $\approx 11\mu m$ (see Methods: Computation of inter-neuron distances, Fig 1B). This difference is more striking when restricted to pyramidal cells (closest neighbor pyramidal cell distance is $\approx 21.3\mu m$ in human versus $\approx 11.5\mu m$ in mouse), as opposed to the distance between interneurons, which is $\approx 28.5\mu m$ in human versus $\approx 22\mu m$ in mouse, due to the higher proportion of interneurons in the human cortex (Fig 1E).

We then computed the expected densities of dendritic branches within the tissue of the two species. For this experiment, we used the number of synapses ($11.8 \times 10^8/mm^3$ in human versus $26.56 \times 10^8/mm^3$ in mouse) within a volume of $1mm^3$ of the cortex (DeFelipe et al., 2002) and the reported synaptic densities (Loomba et al., 2022), $0.88/\mu m$ in human versus $2.15/\mu m$ in mouse). This analysis revealed that the anticipated total length of dendrites per cubic millimeter is comparable between the two species, with human dendrites measuring $\approx 1340m/mm^3$ compared to $\approx 1240m/mm^3$ in mice (Fig 1C), despite their significant dif-

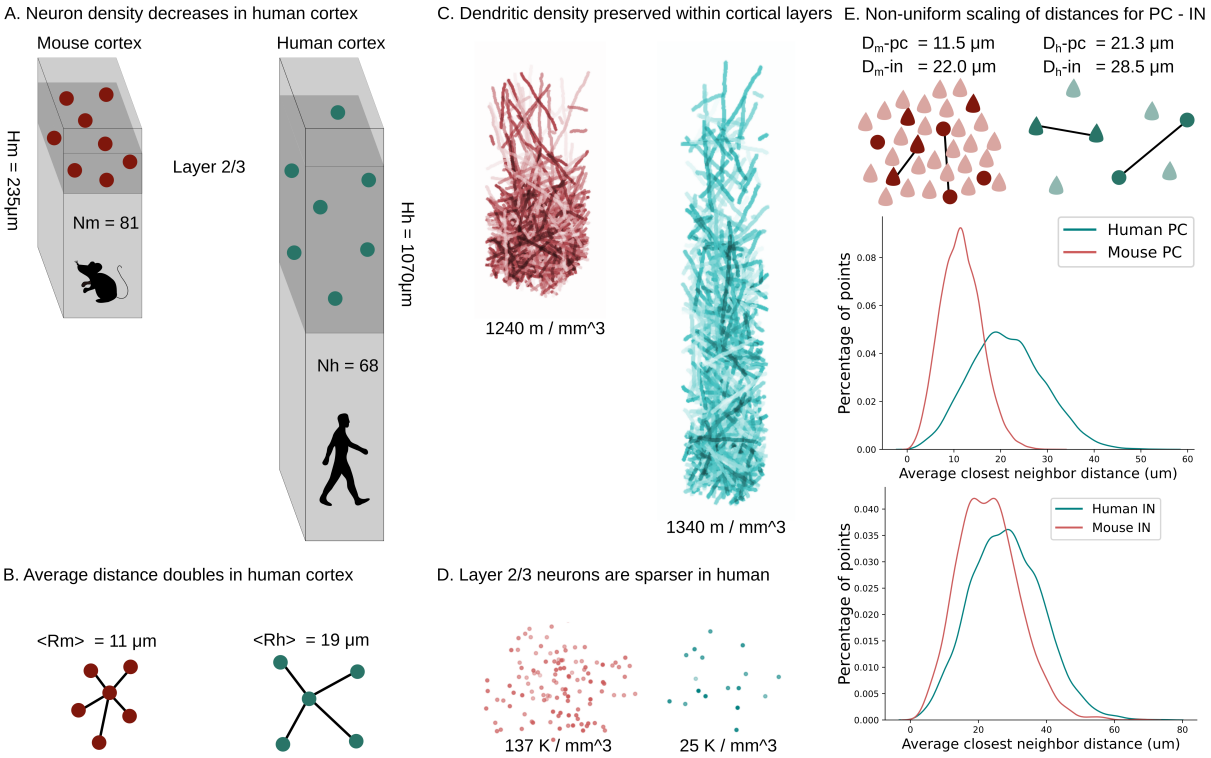

Figure 1: **Comparative analysis of network architecture.** A. Lower neuron density in human cortex leads to increased inter-neuron distances. B. The minimum distance between a pair of neurons is two times greater in humans. C. The density of dendritic branches within the cortical column is preserved between species. D. Due to the higher percentage of interneurons and lower neuron density, pyramidal cells are sparser in humans. E. The average closest neighbor distances between human and mouse neurons are much more striking in pyramidal cells (top) compared to interneurons (bottom), due to the higher proportion of interneurons in the human cortex.

ferences in cell density ($25.7K$ neurons $/mm^3$ in humans versus $137.6K$ neurons $/mm^3$ in mouse).

Layer 2 and 3 human pyramidal cells have larger dendrites and higher dendritic density around the soma

A comprehensive comparative analysis of morphological characteristics between the pyramidal cells of cortical layers 2 and 3 of the two species revealed profound differences between human and mouse neurons and confirmed findings reported in previous studies (Deitcher et al., 2017; Benavides-Piccione et al., 2019). We collected morphologies from diverse sources (Mohan et al., 2015; Deitcher et al., 2017; Benavides-Piccione et al., 2019; Berg et al., 2021).

To ensure the coherence of the datasets, we conducted rigorous assessments to determine if the variation between datasets from different sources was comparable to the variation observed within each individual group. Neurons were selected exclusively from analogous brain regions and within comparable age ranges. The datasets employed for our analysis consisted of mouse and human pyramidal cells (see Fig 2 from the temporal cortex (layers 2, 3 and 5) and hippocampus and interneurons from the layers 2 and 3 cortex (see SI: Datasets). Initially, we focused on pyramidal cells from layers 2 and 3.

Human pyramidal cells are larger, evidenced by their increased total lengths both in apical ($5975 \pm 2697\mu m$ in human apical dendrites, versus $2647 \pm 1047\mu m$ in mice) and basal dendrites ($5616 \pm 4000\mu m$ in human basal dendrites, versus $3127 \pm 1047\mu m$ in mice). The similar dendritic density of the two species, in combination with the significantly lower neuron densities (see Human cortex has lower neuronal density and larger inter-neuron distances), explains the observed greater total length of human dendrites ($11600\mu m$ in human versus $5700\mu m$ in mouse). In addition, human neurons extend to larger distances ($698 \pm 276\mu m$) compared to mouse ($349 \pm 96\mu m$). These differences can be attributed to the increased thickness of the human cortex (2.2 times larger) and the considerably greater thickness of layer 2/3 (4.5 times larger than that of mice) in comparison to the mouse cortex. Additionally, human apical dendrites possess more branches (53 ± 19 in humans, versus 35 ± 11 in mice) and exhibit greater maximum diameters ($8.5\mu m$ in humans, versus $5.9\mu m$ in mice) but smaller overall average diameters ($0.68\mu m$ in human, versus $0.76\mu m$ in mice). The detailed morphological analysis is summarized in Tables S1-S3. The comprehensive morphological analysis uncovered a correlation between neuronal size and cortical depth.

To address this depth effect, cells from different cortical depths were paired with their closest counterparts, ensuring the normalization of cortical depth for subsequent analyses (see Fig 2D). The topological morphology descriptor (TMD, (Kanari et al., 2018)), which encodes the topology of branches at different path distances from the soma, was used to study how branches are distributed in the two species. The extracted topological barcodes of the human (see Fig 6) and mouse (see Fig 7) pyramidal cells unveiled a fundamental difference in their branching patterns (Fig 2G). In the vicinity of the soma, human dendrites exhibit a higher density of branches (Fig 2E), which were also found to be longer than their mouse counterparts. Specifically, dendritic branches of human pyramidal cells start closer to the soma ($200 - 400\mu m$, Fig 2F) but extend to larger radial distances, thus conferring a distinct topological profile of longer branches close to the soma to human neurons.

Scaling laws cannot sufficiently explain species-specific phenotypes

We then investigated whether a scaling law might determine the relationship between the dendrites of the two species. Based on the observed variations in neuron size (Beaulieu-Laroche et al., 2021) and the conserved transcriptomic features (Hodge et al., 2019) across different species, the existence of a scaling law governing these differences has been hypoth-

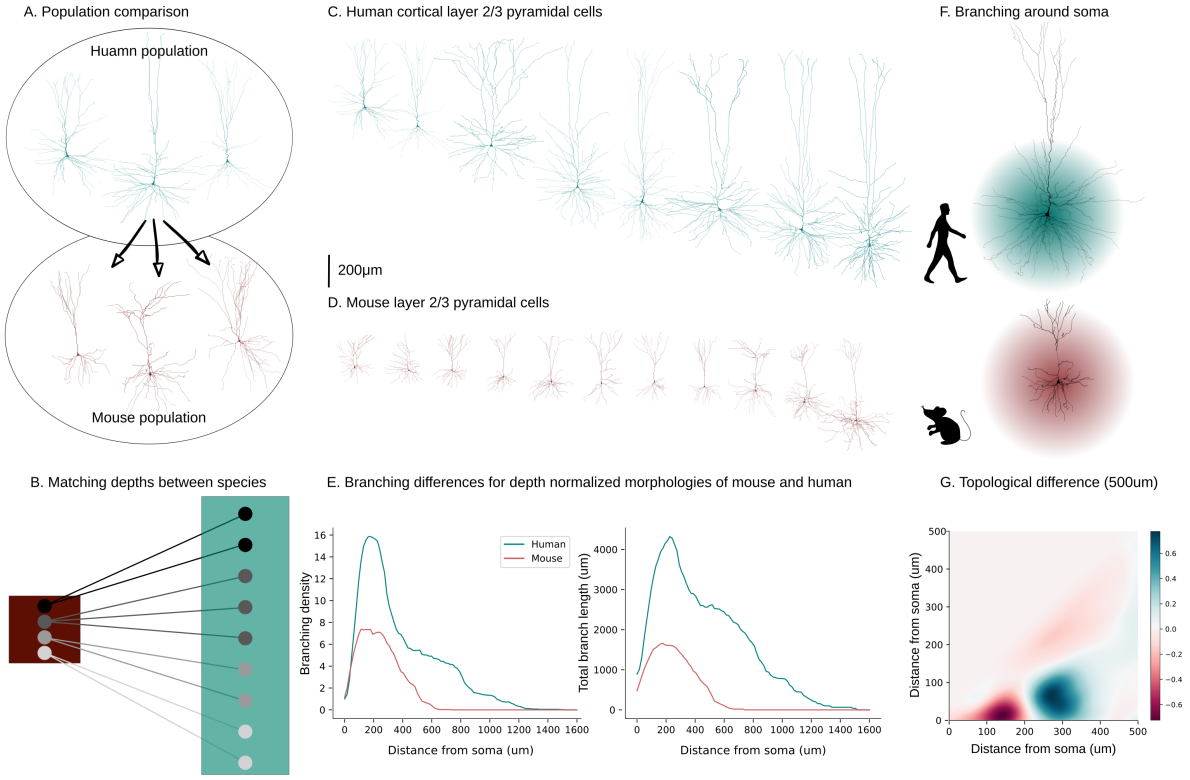

Figure 2: **Comparative topological analysis of layer 2 and 3 cortical pyramidal cells reveals higher branching density around the soma in humans than in mice.** A. Schematic representation of the population comparison approach. B. To ensure accurate comparisons, a process to match cortical depths between the two species was implemented. C. Exemplary reconstructions of layer 2 and 3 cortical pyramidal cells in humans. D. Exemplary reconstructions of layer 2 and 3 cortical pyramidal cells in mice. E. The topological analysis revealed significant differences in branching density between human and mouse pyramidal cells, particularly in the vicinity of the soma, where human pyramidal cells exhibited more (left) and longer (right) branches. F. Example morphologies of human (top) and mouse (bottom). Circles of the same diameter around the soma highlight the difference in branching within this region. G. Zoom-in of the difference in persistence images around the soma indicating that the area of maximum difference is localized at $200 - 500\mu m$.

esized. Single-nucleus RNA-sequencing analysis conducted in both species (Hodge et al., 2019; Berg et al., 2021; Bakken et al., 2021) demonstrated a conserved identity of molecular cell types, with expected varied characteristics within each type, suggesting a similar trend may be anticipated in terms of morphological types.

In an attempt to identify a potential scaling law, we discovered that the distinct topolog-

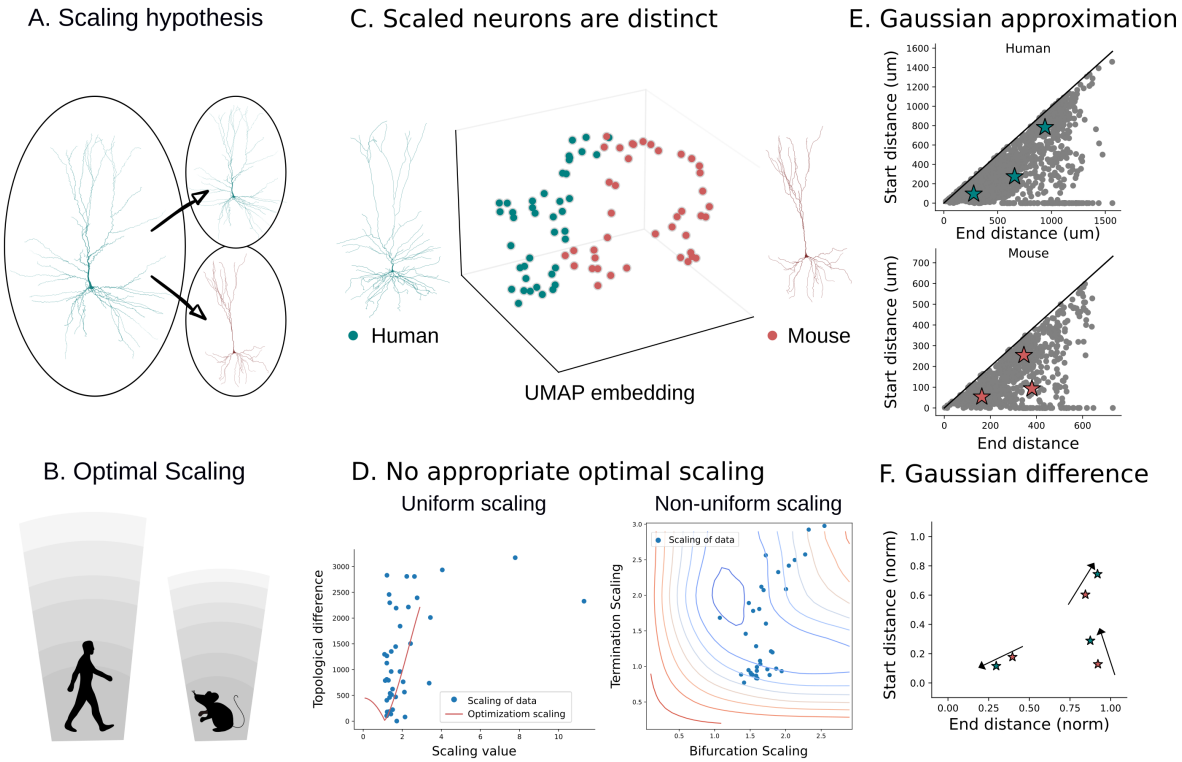

Figure 3: **Scaling laws cannot sufficiently explain species-specific phenotypes.** A. Schematic representation of the scaling hypothesis to explore the feasibility of a suitable scaling law. B. Schematic of the scaled cortical thickness between the two species. C. The UMAP embedding of the topological representations (normalized to total extents) of human (teal) and mouse (red) neurons shows a distinction between the two species. D. Comparison of computed optimized scaling. Neither uniform (red curve, left) nor non-uniform (contour, right) scaling can explain experimental data. E. Persistence diagrams represent the start and end radial distances of branches from the soma. Gaussian kernels (3 centers) are used to approximate the density of topological branching within the persistence diagrams (in gray) of the two species. F. The optimal transformations of the three Gaussian kernels to convert the normalized persistence diagrams from mouse to human are not aligned, indicating the absence of a consistence transformation between the species.

ical characteristics of human cells prevent the formulation of a simplistic description of the interspecies differences. The high density of dendritic branches near the somata of human neurons, combined with relatively comparable branch numbers at greater distances from the soma, necessitates a more complex description to elucidate the observed disparities. Human and mouse dendrites exhibit significant differences that cannot be reconciled by a simple

scaling law. A UMAP embedding (McInnes et al., 2018) of the human and mouse topological barcodes, appropriately scaled to compensate for the observed differences in the cortical thickness between the two species,(Fig 3C) demonstrates that the two species are clearly distinct. Therefore, characteristics beyond relative sizing should be taken into account in a comprehensive description of the species differences.

By employing an optimization algorithm to minimize the distances between mouse and human persistence barcodes, we showed that neither uniform nor non-uniform scaling (see Fig 3D, Methods: Scaling optimization) could adequately fit the experimental data. By approximating the persistence diagrams by a Gaussian kernel (three centers, Fig 3E), we demonstrated that the distinct density patterns observed at different distances from the soma are specific to each species, a property that explains why a simple scaling law cannot sufficiently approximate the data (Fig 3F).

Topological profiles of pyramidal cells show species-specific morphological traits that are universal in multiple brain regions

The topological analysis was generalized to other cortical layers (layer 5) and brain regions (hippocampus) for which data were available. The topological examination of pyramidal cells from the layer 5 temporal cortex revealed the persistence of observed topological differences in deeper cortical layers. The dendritic branches of layer 5 human pyramidal (Fig 8) cells exhibited a higher density in proximity to the soma, with branches commencing earlier and extending further away from the soma than in mouse, confirming that the observed topological profiles of human cells extend to neurons beyond layers 2 and 3.

Remarkably, these results generalize to other brain regions. Data obtained from Benavides et al (Benavides-Piccione et al., 2019) in the mouse and human hippocampus (Fig 8) demonstrated a similar pattern. This finding is particularly intriguing as it highlights a distinct single-cell characteristic that serves as a signature feature of human cells, with high branch densities localized at $200 - 500\mu m$ around neuronal somata.

A topological analysis was also performed on the basal dendrites of interneurons in layers 2 and 3 for human and mouse (Fig 9). The results of this analysis demonstrated that the observed topological differences between the two species persist in the dendrites of interneurons (Fig 9). Specifically, we observed a higher density of dendritic branches surrounding the soma of human interneurons, similar to the pyramidal cells. However, these differences were not as significant as in the pyramidal cells, with fewer branches that extend to smaller distances from the soma than in pyramidal cells.

This distinct topological pattern highlights a clear differentiation between pyramidal cells and interneurons within the cortical circuitry. These findings further emphasize the complexity and diversity of neuronal architecture in the human brain and suggest that different cell types contribute to the overall network organization in distinctive ways.

Increased memory capacity stems from increased dendritic complexity

The natural question that follows is whether the observed structural differences confer a computational advantage to the human brain. Numerous studies have supported the importance of dendritic complexity for computational capacity (Segev, 1998; Koch and Segev, 2000; Häusser and Mel, 2003; Larkum, 2022). To address this question, we build upon the work by Poirazi and Mel (Poirazi and Mel, 2001) by calculating the anticipated memory capacity for a non-linear branching dendrite and comparing it with its topological complexity (Fig 10). Memory capacity is defined as the number of possible combinations between the inputs of the dendrite and its non-linear components (see Methods Memory capacity). Topological complexity, in this context, refers to the entropy of bar lengths within the persistence barcode of a neuron (see Methods: Topological analysis). We observed that memory capacity is correlated with topological complexity (Fig 10), as anticipated by the increased number of branches, enabling the sampling of a larger combination space for the synaptic inputs. The topological complexity of human pyramidal cells is greater than that in mice by a factor of 1.8, resulting in a corresponding enhancement in memory capacity by a factor of 1.7. These findings suggest that dendritic complexity serves as a suitable indicator for predicting the expected memory capacity of individual neurons.

Human pyramidal cells generate strongly connected subnetworks

Our study also delved into the influence of dendritic topology and neuron density on the networks in human and mouse brains, exhibiting significant differences between the two species. Based on neuron densities, we computed the number of neurons at varying distances from a central neuron (Fig 4A-B). This analysis revealed a significantly lower number of neighboring neurons surrounding human somata than in mice. This difference in the predicted number of neighbors is especially remarkable within the range of $200 - 500um$, a property that is expected to highly influence the connection probability between neurons.

A computation of pairwise connectivity at varying distances between pre-synaptic and post-synaptic cells (Fig 4C) disclosed a higher number of appositions, i.e., touches that can potentially become synapses, in human cells than in mouse cells. Interestingly, when a similar analysis was conducted on mouse cells scaled to twice their original extents, fewer appositions were observed, an effect that can be attributed to the increased empty space between branches. Hence, the spatial arrangement of branches and their topological organization around the soma are crucial factors in neuronal connectivity. The higher perisomatic branch density seems to be an essential feature to ensure sufficient connectivity between pairs of human neurons, as computed in (Hunt et al., 2022), compensating for the smaller number of neighbors around a neuron than in mice.

In order to investigate the combined effect of neuronal density and morphology on the

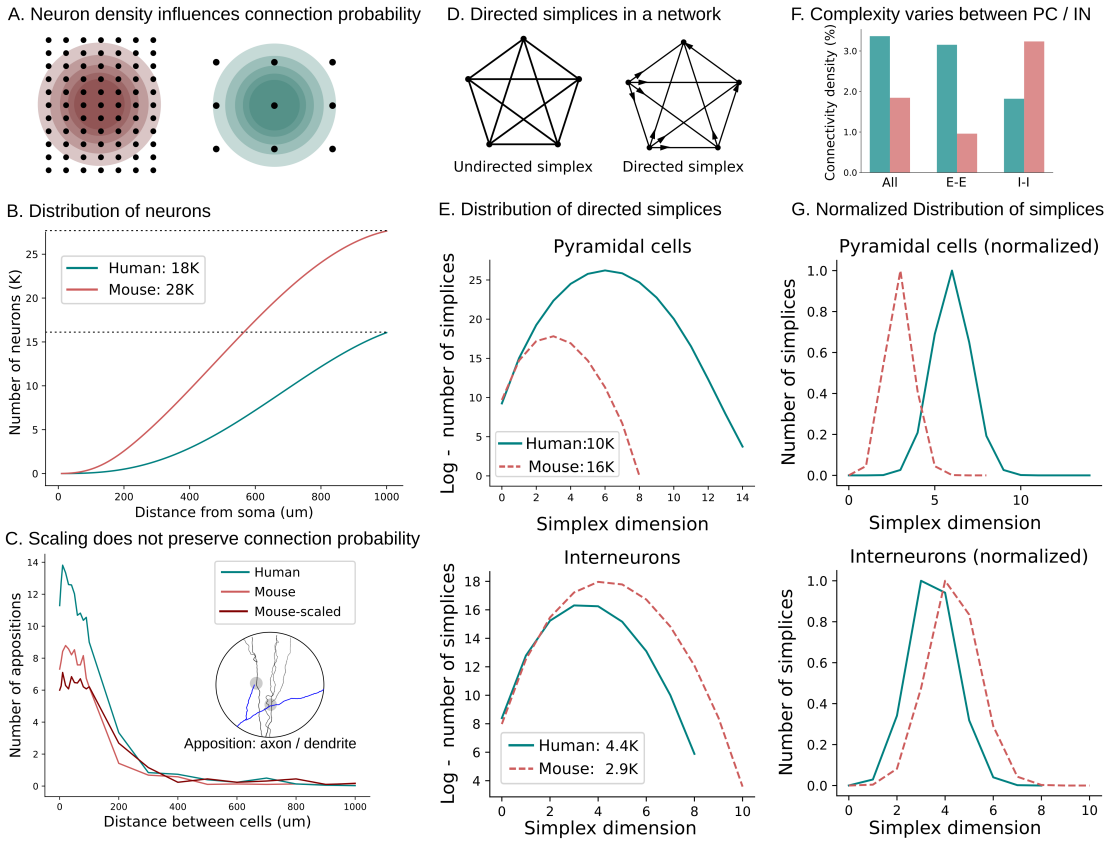

Figure 4: **Human pyramidal cells generate strongly connected subnetworks.** A. Grid illustrating differences in neuron density in human (teal) and mouse (red). Concentric spheres surrounding a central neuron portray the cell counts presented in (B). B. Predicted number of neighbors. A cortical layer 2/3 of dimensions $1mmx1mm$ was simulated for the respective cortical thickness of mouse ($235\mu m$) and human ($1070\mu m$) and the respective neuron counts for mouse ($28K$) and human ($18K$). The number of neurons at different distances ($0 - 1000\mu m$) from a central neuron is computed. Insert reports total cell counts. C. Number of pairwise appositions between human (teal), mouse (red) and scaled mouse (deep red) pyramidal cells. Insert illustrates apposition between a human pre-synaptic axon and the post-synaptic dendrite. D. Example of a five-simplex in undirected and directed graphs. E. Distribution of simplices of different dimensions for pyramidal cells (top) and interneurons (bottom). Insert reports cell counts. Note that cell counts do not reflect cell density due to the differences in the cortical volumes. Log-scale is used for the number of simplices to depict the 3 orders of magnitude higher simplex counts in human. F. Density of connectivity matrices for all connections and excitatory, inhibitory sub-graphs. G. Normalized distributions of simplices, to exhibit the higher dimension of human pyramidal cell networks, in particular the existence of fully connected sub-graphs with up to 15 nodes.

connectivity of a network, we generated sample cortical layers 2/3 for both human and mouse. Using available data on neuronal densities (DeFelipe et al., 2002) and the ratio of excitatory to inhibitory neurons (Loomba et al., 2022), along with morphological reconstructions for four different cell types (human pyramidal cells, mouse pyramidal cells, human interneurons, and mouse interneurons, see SI: Datasets), we calculated the connectivity of the simulated human and mouse circuits. It is important to note that the connectivity was determined through a random selection of 50% of the appositions, and thus, no direct comparison can be made to the connectivity measurements observed in actual biological circuits. We observed a higher connectivity density, i.e. the ratio between the actual connections in the network over the maximum number of possible connections, within the human pyramidal cells subgraph (Fig 4F) than in the comparable graph for mice. On the other hand, the respective connectivity density of human interneurons is lower, despite the higher interneuron density in the human cortex ($4.4K/mm^3$ in humans versus $3K/mm^3$ in mice) and the lower pyramidal cell density ($10K/mm^3$ in human versus $16K/mm^3$ in mouse).

The complexity of the respective networks was assessed by computing the distribution of directed simplices (Reimann et al., 2017). Simplices provide a comprehensive representation of fully connected subgraphs within the networks (Fig 4D), combining information about the density and the degree distribution of the graphs and represent network hubs that are related to modulation of cortical dynamics (Gal et al., 2021). Furthermore, it is worth noting that higher-dimensional simplices are associated with increased robustness in networks (Nolte et al., 2019), since information can be efficiently transmitted in a specific direction, as all edges within the simplices are aligned to transmit information in the same direction.

In particular, we compared the distributions of directed simplices in the human and mouse networks of pyramidal cells and interneurons. Surprisingly, despite the lower neuronal density observed in the human layer 2/3 cortex, the sub-network of pyramidal cells exhibited a complex connectivity pattern, leading to the formation of higher-dimensional simplices. Specifically, in the human network, we observed simplices of dimension 15, whereas, in the mouse network, the dimension was limited to 9 (Fig 4E,G). The number of simplices in the human network was approximately three orders of magnitude larger compared to the mouse network. These findings suggest that the human cortical network displays a greater degree of complexity than its mouse counterpart, despite the lower neuronal density. These results do not generalize to the network of interneurons. The I/E ratio is larger in human (30% in human versus 12% in mouse), however the density of interneurons (cell counts per volume) is still lower in human ($7.7K/mm^3$ in human versus $16.5K/mm^3$ in mouse). In addition, because the topological complexity of human interneurons is only marginally higher than mouse (Fig 9D-F), interneuron networks exhibit lower dimensional simplices (9 in humans versus 11 in mice) and smaller simplex counts, further demonstrating the substantial impact of cell morphology on the overall network organization.

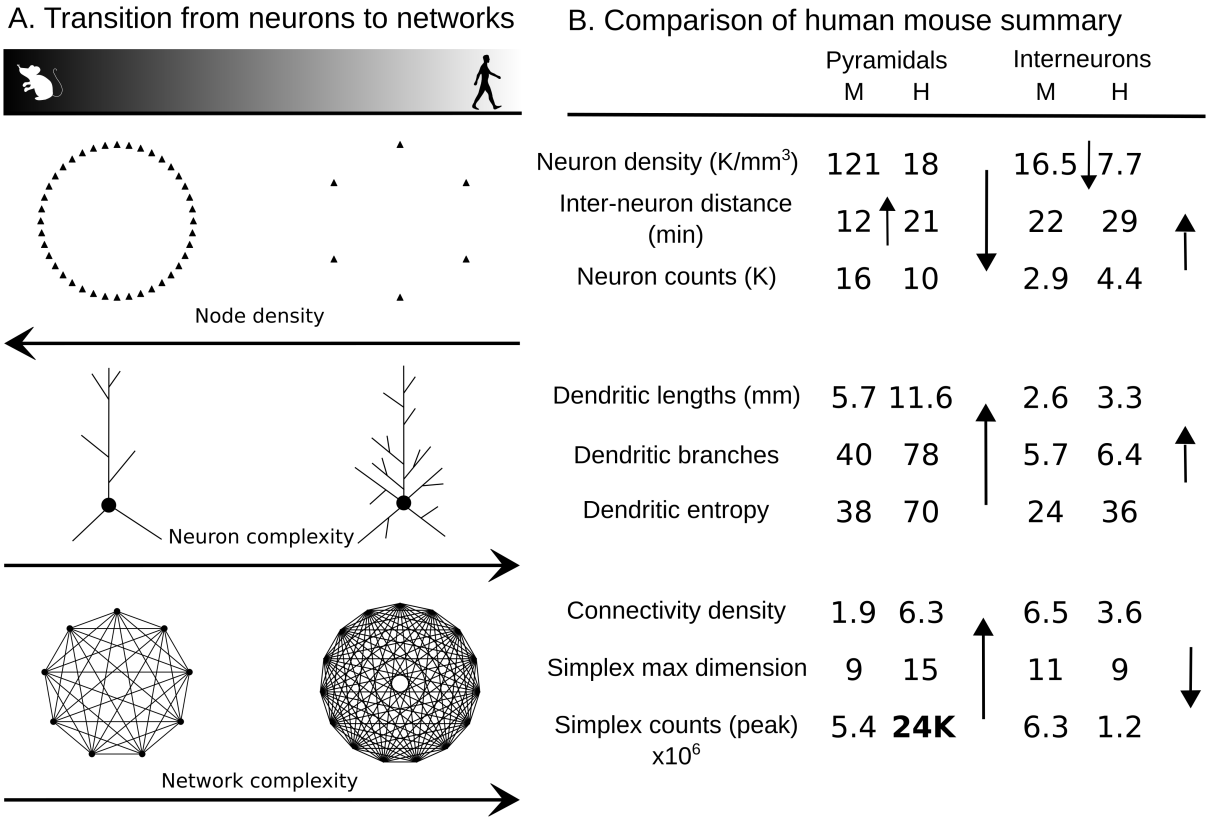

Figure 5: **Single-cell complexity influences networks complexity.** A. The complex dendrites of human pyramidal cells compensate for the lower neuronal density and the increased inter-neuron distances to generate networks with numerous highly connected sub-graphs. Network complexity depends on dendritic complexity more strongly than on neuronal density. B. Summary of differences between human and mouse, for excitatory (pyramidal cells) and inhibitory cells (interneurons). While lower neuronal density in humans leads to greater distances between neurons, the over-representation of interneurons in humans mitigates this difference. Human pyramidal cells exhibit significantly higher dendritic complexity than in mice, whereas interneurons display only a modest increase in complexity. Consequently, the sub-network of human pyramidal cells comprises substantially more all-to-all connected subgraphs, composed of significantly more nodes, as evidenced by the notably higher simplex counts than in mice ($5K$). On the contrary, the sub-network of interneurons exhibits somewhat lower simplex counts than in mice.

Cognitive enhancement hypothesis

Despite the greater inter-neuron distances resulting from lower neuron density in human pyramidal cells, the distinct topology of their dendritic arbors emerges as a mechanism to establish higher-order interactions, as evidenced by the larger number of higher-dimensional

simplices in the network. In contrast, while interneurons exhibit higher densities in human, their simpler structural characteristics limit their capacity to enhance network complexity to the same extent. These observations are supported by a balance in inhibition and excitation (Loomba et al., 2022) in the innervation of pyramidal cells in the human cortex. These findings suggest that the intricate morphology of individual neurons can significantly influence the properties and characteristics of the networks they contribute to, providing strong evidence of a direct link between dendritic complexity and the overall structure of neuronal networks.

Two primary approaches to achieve higher-order complexity in neuronal networks are commonly proposed: increasing the number of nodes (Jang et al., 2020) or enhancing the complexity of individual nodes (Zhang and fei Qiao, 2010; Pagkalos et al., 2022). Interestingly, instead of simply adding more nodes, the human brain has evolved to prioritize the complexity of individual neurons, as observed in the morphological characteristics of human pyramidal cells. This suggests that the human brain has harnessed the potential of single-neuron complexity as a mechanism to create and support complex network connectivity, potentially conferring unique cognitive advantages.

Discussion

Topological analysis of human and mouse neurons revealed significant morphological differences between the two species. In particular, dendrites of human pyramidal cells exhibit a higher density of branches around the soma ($200 - 500\mu m$) than mouse dendrites. The observed topological differences persist across cortical layers (layers 2, 3 and 5) and brain regions (hippocampus), suggesting they are a defining feature of human cells. We found that the distinctive perisomatic branching pattern exhibited by human dendrites serves as an effective compensatory mechanism for the increased inter-neuron distance, in order to preserve the density of dendritic processes and the connectivity between neurons.

Furthermore, the higher dendritic complexity in humans contributes to substantially higher numbers and dimensions of simplices in networks of human pyramidal cells, suggesting that dendritic morphology has considerable influence on how individual cells interconnect to form a network. The increased structural complexity generated by the sophisticated shapes of dendrites suggests that a network is not merely a simple sum of its individual components. The intricate branching patterns of human pyramidal cells potentially enable more robust and coordinated neural computations through the formation of highly coordinated sub-networks, represented by higher dimensional simplices. This result reinforces the view that dendritic complexity plays a crucial role in biological networks (Häusser and Mel, 2003; Larkum, 2022).

Our analysis substantiates a compelling hypothesis that challenges the conventional notion of increasing node density as a means of optimizing the computational capacity of

networks. Instead, we propose that enhancing node complexity, as observed in the distinct morphological features of human neurons, may be an alternative mechanism for optimizing network performance. The biological mechanism by which increased node complexity enhances the computational capabilities of a network remains an intriguing open question. However, it is not difficult to imagine that the simultaneous greater memory capacity within individual neurons and the substantially higher simplex counts should result in networks with higher computational power. As our understanding of the human neocortex continues to evolve, we anticipate that future models of the human cortex will integrate comprehensive information about cell types, transcriptomic and morpho-electrical relationships (Bakken et al., 2021; Berg et al., 2021), and preferential connectivity rules (Kalmbach et al., 2021; Loomba et al., 2022) to create a more accurate understanding of the human brain.

The interplay between interneurons and pyramidal cells, as well as the functional role of each component within the network, is an important aspect that warrants further investigation. With the discovery of a larger proportion of interneurons in the human brain than in mouse, there has been speculation that they may have unforeseen functional significance (Loomba et al., 2022). Our findings suggest that the simpler dendritic shapes of interneurons may necessitate a higher abundance of these cells in order to maintain the balance between excitation and inhibition within the network. Moreover, the sparsity of connections within the interneuron subnetwork implies that their role might primarily involve regulating the highly connected network of pyramidal cells. However, due to the great diversity in interneuron shapes (Chartrand et al., 2022; Lee et al., 2022) and the specific roles of different types in the functionality of human networks (Yao et al., 2021) a more detailed analysis is required. Therefore, exploring the connectivity patterns within the overall network of both excitatory and inhibitory cells, rather than focusing solely on their respective subnetworks, would provide valuable insights into the necessity for a greater number of interneurons and their specific contributions to network dynamics (Yao et al., 2021).

Methods

Topological analysis

Algebraic topology provides mathematical tools to characterize geometric shapes by encoding features that persist across length scales. The Topological Morphology Descriptor (TMD, (Kanari et al., 2018)) represents the branching structure of trees as a persistence barcode, encoding the start and end distances from the soma of each branch in the underlying structure as an interval in the real line.

Given a rooted tree T with a set of N branches that consist of terminations or leaves l and intermediate branching points or bifurcations b, and given a real-valued function f on the nodes of the tree, such as the Euclidean (or path) distance from the root R, the TMD

algorithm generates a persistence barcode PB:

$$PB = \{(b_i, t_i) \mid i \leq N\} \tag{1}$$

Each bar (b_i, t_i) in the persistence barcode associates a branch in the tree T with a pair of real numbers: if the i^{textth} branch has bifurcation b and leaf l, then $b_i = f(b)$ and $t_i = f(l)$.

In brief, the persistence barcode is a set of intervals that encode the values of the function f at the start b and the end l of each branch. An equivalent representation of the persistence barcode is the corresponding persistence diagram PD, in which each interval of the barcode is encoded by the pair of its endpoints, seen as a point in the real plane.

There are many well known methods to generate vectorizations of persistence barcodes, from which one can then compute various statistics. For example, the persistence diagram can be converted to a finite-dimensional vector representation, the persistence image PI (Adams et al., 2015), which is essentially a sum of Gaussian kernels centered around the points in the persistence diagram.

Another useful vectorization of a persistence diagram or barcode is its topological entropy (Chintakunta et al., 2015), which is computed from the lengths of the bars:

$$E(PB) = -\sum_{i}^{N} \frac{l_i}{L} \cdot log(\frac{l_i}{L}) \tag{2}$$

where $l_i = |t_i - b_i|$ is the length of each bar and $L = \sum_i^L l_i$ is the total length of all bars.

Topological scaling

The TMD associates a persistence diagram to any tree and thus to any reconstructed neuron morphology. Re-scaling a tree transforms the associated persistence diagram as follows. If T is a tree with a corresponding persistence barcode $PB = \{(b_i, t_i) \mid i \leq N\}$ given by the affine function f, the tree T' is obtained from T by linear, or uniform, scaling by a factor $\alpha > 0$ of all the branches, then its associated persistence barcode PB' is

$$PB' = \{(\alpha \cdot b_i, \alpha \cdot t_i) \mid i \leq N\}.$$

Note that the persistence entropy is scale-invariant as shown:

$$E(a \cdot PB) = -\sum_{i}^{N} \frac{a \cdot l_i}{a \cdot L} \cdot log(\frac{a \cdot l_i}{a \cdot L}) = -\sum_{i}^{N} \frac{l_i}{L} \cdot log(\frac{l_i}{L}) = E(PB) \tag{3}$$

If T is a tree with a corresponding persistence barcode PB as above, and the tree T'' is obtained from T by scaling by a pair of factors $\alpha, \beta > 0$ of all the branches, so that the bifurcations of the branches are scaled by α and the leaves by β, then its associated persistence barcode PB'' is

$$PB'' = \{(\alpha \cdot b_i, \beta \cdot t_i) \mid i \leq N\}.$$

Scaling optimization

In order to evaluate the scaling hypothesis, we have designed two experiments: the first one assumes uniform scaling through the morphology, and the second one non-uniform scaling as described above.

As a measure of the distance between two populations of cells, we computed the sum of the differences between the persistence images of the two populations, where the persistence image of a population is the sum of the persistence images of each cell in the population.

In the case of uniform scaling, we sought an optimal scaling factor $\alpha > 0$ that transforms the population of mouse cells to human cells, minimizing the distance between the two populations.

For the non-uniform scaling, we sought for two independent scaling factors $\alpha > 0$ and $\beta > 0$ to transform the population of mouse cells to human cells, minimizing the distance between the two populations.

In both cases, a gradient descent approach was implemented to identify the optimal factors. The results are presented in Fig 3D, along with the respective experimental data for comparison. Even though the identified optimal factors minimize the topological distances (difference between persistence images) between the two populations, they cannot capture the individual data points.

Computation of inter-neuron distances

The inter-neuron distances were computed in two ways: by a mathematical formula and by a simulation of points generated according to the selected density and the respective spatial dimension. For the mathematical formula, we used equation (4) from (Bansal and Ardell, 1971).

$$< R_v >= 0.554 \times N_v^{-1/3} \tag{4}$$

where $N_v = \frac{N}{V}$ is defined as the number of particles N per unit volume V.

The result was confirmed by the computational generation of 100 instances of uniform point processes and computing the average minimum distance within each set of points. The reported results correspond to the distance computed by the simulation, but the computation using the mathematical formula (4) yielded the same values.

Density of dendritic branches

Based on the total number of synapses within a cortical volume S_v and the density of synapses d_{syn} on the dendrites, the density d_{dend} of dendritic branches within a cortical volume is computed as:

$$d_{dend} = \frac{S_v}{d_{syn}} \tag{5}$$

Similarly, the density of axons can be computed by the bouton density d_{bouton}:

$$d_{axon} = \frac{S_v}{d_{bouton} * n_{syn_bouton}} \tag{6}$$

However, due to inconclusive experimental data about the number n_{syn_bouton} of synapses that correspond to each bouton, we were unable to provide an accurate measurement for the respective axon density.

In addition, the measurements of axonal lengths and bouton densities for individual neurons are difficult to assess experimentally, due to the inability of staining techniques to accurately stain the axonal processes that are further away from the soma. Therefore, the analysis of axonal data should be re-assessed once more accurate experimental data become available.

Memory capacity

In (Poirazi and Mel, 2001) the memory capacity is computed based on two different models: the linear model, which assumes dendritic inputs are summed linearly at the neuronal soma, and the non-linear model, which assumes the dendritic branches integrate the signal non-linearly. Independent of the choice of non-linearity introduced on the dendrites, memory capacity increases significantly if non-linearities are taken into account.

Given a dendrite with m branches, each branch contains k excitatory inputs, thus $s = mk$ synaptic contacts and a set of d dendritic inputs, the memory capacity can be computed as follows.

For the linear model, the computed memory capacity is:

$$C_L = 2log_2\binom{s+d-1}{s} \tag{7}$$

Note that in this case, the number of branches m and their synaptic length k are not relevant for the computation of the memory capacity.

For the non-linear model, the computed memory capacity is:

$$C_N = 2log_2\binom{\binom{k+d-1}{k}+m-1}{m} \tag{8}$$

On the contrary, for the non-linear model, the distribution of synaptic lengths k on the m branches plays a crucial role in the memory capacity of the dendrite. As shown in Fig 10B the memory capacity increases with the number of branches, due to the increased number of ways to combine the dendritic inputs. The number of branches here corresponds to the number of computational subunits in the dendritic tree (Polsky et al., 2004), rather than the physical branches of the tree.

Computation of appositions

The appositions between a pair of neurons were quantified as the number of "contact points" where the pre-synaptic axons approach the post-synaptic dendrites within a distance of $2\mu m$. It is important to note that these contact points do not directly represent synaptic connections, but rather indicate potential sites for synapse formation. Therefore the results presented on appositions should be interpreted as a measure of the likelihood of synaptic connections between neurons.

The detailed methodology for the computation of the appositions is described in (Reimann et al., 2017).

Computation of simplex distribution

Recent advances in algebraic topology (Sizemore et al., 2016; Reimann et al., 2017) have introduced a powerful tool for comprehending network complexity - the computation of cliques and cavities formed by the underlying graph. This approach allows for a deeper understanding of the intricate connections and structures within networks, enabling researchers to unveil hidden patterns and gain insights into their organizational principles.

The dimension of a clique in a network is one less than the number of neurons of which it is composed; higher dimensions indicate higher complexity. In directed graphs, directed cliques are of particular significance as they comprise a single source neuron and a single sink neuron, representing a distinct pattern of connectivity, with the potential to influence the flow of activity within the network, making it an important consideration in network analysis (Perin et al., 2011; Nolte et al., 2019).

To bring the connection probability within a reasonable range, we applied a random reduction of 50% to the connectivity matrix formed by the appositions between neurons. This adjustment aimed to ensure a more realistic representation of the network by reducing excessive connections. The mouse and human networks were partitioned into distinct excitatory and inhibitory subnetworks. For each subnetwork, we computed the connection probability and analyzed the distribution of simplices, allowing us to assess the network characteristics and topological complexity specific to each subpopulation.

Data availability

The data and the code used in this study will become available upon request after publication. The topological analysis was performed using https://github.com/BlueBrain/TMD. The morphological analysis was performed using https://github.com/BlueBrain/NeuroM.

Author contributions

L.K. conceived and supervised the study, designed the computational experiments, performed analysis, and wrote the manuscript. Y.S. supervised, performed, and validated reconstructed neurons. A.A. analyzed neuronal morphologies and generated neuronal networks. N.B. collected and revised literature information. R.B.P. reconstructed neurons and provided synaptic data for the human and mouse cortex and hippocampus. J.C. edited the manuscript. J.D.F. provided anatomical and connectivity data for the human and mouse cortex. K.H. designed the topological methods and edited the manuscript. H.D.M. provided anatomical data for the human cortex. E.J.M. performed experiments and reconstructed human neurons. I.S. supervised the study. H.M. supervised the study and provided funding. C.P.J.d.K. provided data and supervised the study. All authors reviewed the paper and discussed the results at all stages of this study.

Acknowledgements

The authors thank Daniela Egas-Santader for her useful contributions to the efficient computation of simplices in the generated networks. This study was supported by funding to the Blue Brain Project, a research center of the École polytechnique fédérale de Lausanne (EPFL), from the Swiss government's ETH Board of the Swiss Federal Institutes of Technology.

References

Henry Adams, Tegan H. Emerson, Michael J. Kirby, Rachel Neville, Chris Peterson, Patrick D. Shipman, Sofya Chepushtanova, Eric M. Hanson, Francis C. Motta, and Lori Ziegelmeier. Persistence images: A stable vector representation of persistent homology. *J. Mach. Learn. Res.*, 18:8:1–8:35, 2015.

Trygve E Bakken, Cindy T. J. van Velthoven, Vilas Menon, Rebecca D. Hodge, Zizhen Yao, and Thuc Nghi Nguyen et al. Single-cell and single-nucleus rna-seq uncovers shared and distinct axes of variation in dorsal lgn neurons in mice, non-human primates, and humans. *eLife*, 10, 2021.

P. P. Bansal and Alan J. Ardell. Average nearest neighbor distances between uniformly distributed finite particles. topical report. 1971.

Lou Beaulieu-Laroche, Norma J. Brown, Marissa Hansen, Enrique H. S. Toloza, Jitendra Sharma, Ziv M. Williams, Matthew P. Frosch, G. Rees Cosgrove, Sydney S. Cash, and Mark T. Harnett. Allometric rules for mammalian cortical layer 5 neuron biophysics. *Nature*, 600:274 – 278, 2021.

Ruth Benavides-Piccione, Inmaculada Ballesteros-Yáñez, Javier DeFelipe, and Rafael Yuste. Cortical area and species differences in dendritic spine morphology. *Journal of Neurocytology*, 31:337–346, 2002.

Ruth Benavides-Piccione, Mamen Regalado-Reyes, Isabel Fernaud-Espinosa, Asta Kastanauskaite, Silvia Tapia-González, Gonzalo León-Espinosa, Concepción Rojo, Ricardo Insausti, Idan Segev, and Javier DeFelipe. Differential structure of hippocampal ca1 pyramidal neurons in the human and mouse. *Cerebral cortex*, 2019.

Jim Berg, Staci A. Sorensen, Jonathan T. Ting, Jeremy A. Miller, and Tom Chartrand et al. Human neocortical expansion involves glutamatergic neuron diversification. *Nature*, 598: 151 – 158, 2021.

Osvaldo Cairò. External measures of cognition. *Frontiers in Human Neuroscience*, 5, 2011.

Nicolás Cano-Astorga, Javier DeFelipe, and Lidia Alonso-Nanclares. Three-dimensional synaptic organization of layer iii of the human temporal neocortex. *Cerebral Cortex (New York, NY)*, 31:4742 – 4764, 2021.

Nicolás Cano-Astorga, Sergio Plaza-Alonso, Javier DeFelipe, and Lidia Alonso-Nanclares. 3d synaptic organization of layer iii of the human anterior cingulate and temporopolar cortex. *bioRxiv*, 2023.

Tom Chartrand, Rachel Dalley, Jennie Close, Natalia A. Goriounova, and Brian R. Lee et al. Morpho-electric and transcriptomic divergence of the layer 1 interneuron repertoire in human versus mouse neocortex. *bioRxiv*, 2022.

Harish Chintakunta, Thanos Gentimis, Rocio Gonzalez-Diaz, María José Jiménez, and Hamid Krim. An entropy-based persistence barcode. *Pattern Recognit.*, 48:391–401, 2015.

Javier DeFelipe. The evolution of the brain, the human nature of cortical circuits, and intellectual creativity. *Frontiers in Neuroanatomy*, 5, 2011.

Javier DeFelipe, Lidia Alonso-Nanclares, and Jon I. Arellano. Microstructure of the neocortex: Comparative aspects. *Journal of Neurocytology*, 31:299–316, 2002.

Y. Deitcher, G. Eyal, L. Kanari, M.B. Verhoog, G.A. Atenekeng Kahou, H.D. Mansvelder, C.P.J. de Kock, and I. Segev. Comprehensive morpho-electrotonic analysis shows 2 distinct classes of l2 and l3 pyramidal neurons in human temporal cortex. *Cerebral Cortex (New York, NY)*, 27:5398 – 5414, 2017.

Eyal Gal, Oren Amsalem, Alon Schindel, Michael London, Felix Schürmann, Henry Markram, and Idan Segev. The role of hub neurons in modulating cortical dynamics. *Frontiers in Neural Circuits*, 15, 2021.

AA Galakhova, Sarah Hunt, René Wilbers, Djai B. Heyer, Cpj de Kock, Huibert D. Mansvelder, and Natalia A. Goriounova. Evolution of cortical neurons supporting human cognition. *Trends in Cognitive Sciences*, 26:909–922, 2022.

Michael D. Gregory, J. Shane Kippenhan, Dwight Dickinson, Jessica Carrasco, Venkata S. Mattay, Daniel R. Weinberger, and Karen Faith Berman. Regional variations in brain gyrification are associated with general cognitive ability in humans. *Current Biology*, 26: 1301–1305, 2016.

Benjamin L Hart, Lynette A Hart (Geyer), Michael C. McCoy, and C. R. Sarath. Cognitive behaviour in asian elephants: use and modification of branches for fly switching. *Animal Behaviour*, 62:839–847, 2001.

Michael Häusser and Bartlett W. Mel. Dendrites: bug or feature? *Current Opinion in Neurobiology*, 13:372–383, 2003.

Suzana Herculano-Houzel. The human brain in numbers: A linearly scaled-up primate brain. *Frontiers in Human Neuroscience*, 3, 2009.

Rebecca D. Hodge, Trygve E Bakken, Jeremy A. Miller, Kimberly A. Smith, and Eliza R. Barkan et al. Conserved cell types with divergent features in human versus mouse cortex. *Nature*, 573:61 – 68, 2019.

Michel A. Hofman. Size and shape of the cerebral cortex in mammals. ii. the cortical volume. *Brain, behavior and evolution*, 32 1:17–26, 1988.

William D. Hopkins, William D. Hopkins, Xiang Li, and Neil Roberts. More intelligent chimpanzees (pan troglodytes) have larger brains and increased cortical thickness. *Intelligence*, 2019.

Sarah Hunt, Yoni Leibner, Eline J. Mertens, Natali Barros-Zulaica, and Lida Kanari et al. Strong and reliable synaptic communication between pyramidal neurons in adult human cerebral cortex. *Cerebral Cortex (New York, NY)*, 33:2857 – 2878, 2022.

Jinhyeok Jang, Hyunjoong Cho, Jaehong Kim, Jaeyeon Lee, and Seungjoon Yang. Deep neural networks with a set of node-wise varying activation functions. *Neural networks : the official journal of the International Neural Network Society*, 126:118–131, 2020.

Brian E. Kalmbach, Rebecca D. Hodge, Nikolas L. Jorstad, Scott F. Owen, and Rebecca de Frates et al. Signature morpho-electric, transcriptomic, and dendritic properties of human layer 5 neocortical pyramidal neurons. *Neuron*, 109:2914–2927.e5, 2021.

L. Kanari, P. Dłotko, M. Scolamiero, R. Levi, J. Shillcock, K. Hess, and H. Markram. A topological representation of branching neuronal morphologies. *Neuroinformatics*, 16(1): 3–13, Jan 2018.

Christof Koch and Idan Segev. The role of single neurons in information processing. *Nature Neuroscience*, 3 Suppl 1:1171–1177, 2000.

Matthew Evan Larkum. Are dendrites conceptually useful? *Neuroscience*, 489:4–14, 2022.

Brian R. Lee, Rachel Dalley, Jeremy A. Miller, Tom Chartrand, Jennie Close, and Rusty Mann et al. Signature morpho-electric properties of diverse gabaergic interneurons in the human neocortex. *bioRxiv*, 2022.

Sahil Loomba, Jakob Straehle, Vijayan Gangadharan, Natalie Heike, Abdelrahman Khalifa, Alessandro Motta, Niansheng Ju, Meike Sievers, Jens Gempt, Hanno S. Meyer, and Moritz Helmstaedter. Connectomic comparison of mouse and human cortex. *Science*, 377, 2022.

Leland McInnes, John Healy, Nathaniel Saul, and Lukas Großberger. Umap: Uniform manifold approximation and projection. *J. Open Source Softw.*, 3:861, 2018.

Kyle R Menary, Paul F. Collins, James N. Porter, Ryan L. Muetzel, Elizabeth A. Olson, Vipin Kumar, Michael S. Steinbach, Kelvin O. Lim, and Monica Luciana. Associations between cortical thickness and general intelligence in children, adolescents and young adults. *Intelligence*, 41 5:597–606, 2013.

Hemanth Mohan, Matthijs B Verhoog, Keerthi Kumar Doreswamy, Guy Eyal, and Romy Aardse et al. Dendritic and axonal architecture of individual pyramidal neurons across layers of adult human neocortex. *Cerebral Cortex (New York, NY)*, 25:4839 – 4853, 2015.

Max Nolte, Eyal Gal, Henry Markram, and Michael W. Reimann. Impact of higher order network structure on emergent cortical activity. *Network Neuroscience*, 4:292 – 314, 2019.

Michalis Pagkalos, Spyridon Chavlis, and Panayiota Poirazi. Dendrify: a new framework for seamless incorporation of dendrites in 1 spiking neural networks. 2022.

Rodrigo Perin, Thomas K. Berger, and Henry Markram. A synaptic organizing principle for cortical neuronal groups. *Proceedings of the National Academy of Sciences*, 108:5419 – 5424, 2011.

Panayiota Poirazi and Bartlett W. Mel. Impact of active dendrites and structural plasticity on the memory capacity of neural tissue. *Neuron*, 29:779–796, 2001.

Alon Polsky, Bartlett W. Mel, and Jackie Schiller. Computational subunits in thin dendrites of pyramidal cells. *Nature Neuroscience*, 7:621–627, 2004.

Michael W. Reimann, Max Nolte, Martina Scolamiero, Katharine Turner, Rodrigo Perin, Giuseppe Chindemi, Pawel Dlotko, Ran Levi, Kathryn Hess, and Henry Markram. Cliques of neurons bound into cavities provide a missing link between structure and function. *Frontiers in Computational Neuroscience*, 11, 2017.

Astrid Rollenhagen, Bernd Walkenfort, Rachid Yakoubi, Sarah A Klauke, Sandra F Schmuhl-Giesen, Jacqueline Heinen-Weiler, Sylvia Voortmann, Brigitte Marshallsay, Tayfun Palaz, Ulrike Holz, Mike Hasenberg, and Joachim H. R. Lübke. Synaptic organization of the human temporal lobe neocortex as revealed by high-resolution transmission, focused ion beam scanning, and electron microscopic tomography. *International Journal of Molecular Sciences*, 21, 2020.

Idan Segev. Sound grounds for computing dendrites. *Nature*, 393:207–208, 1998.

Ann E. Sizemore, Chad Giusti, Ari E. Kahn, Jean M. Vettel, Richard F. Betzel, and Danielle S. Bassett. Cliques and cavities in the human connectome. *Journal of Computational Neuroscience*, 44:115 – 145, 2016.

David A Waugh and J. G. M. Thewissen. The pattern of brain-size change in the early evolution of cetaceans. *PLoS ONE*, 16, 2021.

Heng Kang Yao, Alexandre Guet-McCreight, Frank Mazza, Homeira Moradi Chameh, Thomas D. Prevot, John David Griffiths, Shreejoy J. Tripathy, Taufik A. Valiante, Etienne Sibille, and Etay Hay. Reduced inhibition in depression impairs stimulus processing in human cortical microcircuits. *bioRxiv*, 2021.

Zhaozhao Zhang and Jun fei Qiao. A node pruning algorithm for feedforward neural network based on neural complexity. *2010 International Conference on Intelligent Control and Information Processing*, pages 406–410, 2010.

Supplementary

Dataset

- Mouse layer 2/3 Pyramidal cells from temporal association cortex: De Kock
- Mouse layer 2/3 Interneurons from cortex: LNMC, neuromorpho.org
- Mouse layer Pyramidal cells from temporal association cortex: De Kock, LNMC
- Mouse hippocampus Pyramidal cells from temporal association cortex: Behavides
- Human layer 2/3 Pyramidal cells from temporal association cortex: De Kock, Allen Institute
- Human layer 2/3 Interneurons from temporal association cortex: LNMC, Allen Institute
- Human layer Pyramidal cells from temporal association cortex: De Kock
- Human hippocampus Pyramidal cells from temporal association cortex: Behavides

	HL23PC	HL23IN	ML23PC	ML23IN
Num sections	58.92	37.77	47.29	41.35
Num bif	26.30	16.36	19.34	18.52
Num leaves	32.12	21.36	26.89	23.47
Total length	5616.85	3418.25	3127.66	2376.06
Section length	93.13	94.02	65.86	63.46
Mean radii	0.32	0.32	0.34	0.37
Section term length	146.60	142.65	93.99	79.94
Section bif length	25.57	28.32	26.78	36.32
Branch orders	5.05	4.85	4.61	4.78
Path distances	144.89	139.99	107.98	120.63
Radial distances	109.79	106.38	79.26	85.11
Section volume	35.88	43.60	25.19	38.01
Section area	186.18	197.52	140.04	153.98

Table S1: Average morphometrics for basal reconstructions of layers 2 and 3 for mouse (M) and human (H) pyramidal cells (PC) and interneurons (IN).

	HL23PC	HL23IN	ML23PC	ML23IN
Num sections	52.60	0.00	36.71	0.00
Num bif	25.32	0.00	16.76	0.00
Num leaves	26.93	0.00	18.92	0.00
Total length	5975.23	0.00	2647.04	0.00
Section length	112.98	0.00	73.04	0.00
Mean radii	0.34	0.00	0.38	0.00
Section term length	165.57	0.00	98.19	0.00
Section bif length	57.68	0.00	47.77	0.00
Branch orders	11.66	0.00	8.39	0.00
Path distances	299.20	0.00	235.09	0.00
Radial distances	242.67	0.00	184.45	0.00
Section volume	52.41	0.00	36.17	0.00
Section area	242.42	0.00	172.63	0.00

Table S2: Average morphometrics for apical reconstructions of layers 2 and 3 for mouse (M) and human (H) pyramidal cells (PC) and interneurons (IN).

	HL23PC	HL23IN	ML23PC	ML23IN
Num sections	29.07	181.31	1.48	292.31
Num bif	37.80	99.14	1.17	141.20
Num leaves	15.06	91.16	1.24	148.21
Total length	3894.02	11923.42	337.63	14061.91
Section length	115.98	73.17	279.72	51.42
Mean radii	0.21	0.10	0.26	0.07
Section term length	134.96	85.68	280.25	62.11
Section bif length	80.63	57.54	128.20	40.33
Branch orders	11.02	16.60	1.17	20.42
Path distances	226.07	406.96	297.93	355.17
Radial distances	150.25	167.54	272.67	128.09
Section volume	58.03	3.51	68.38	1.06
Section area	208.35	47.31	464.91	21.16

Table S3: Average morphometrics for axonal reconstructions of layers 2 and 3 for mouse (M) and human (H) pyramidal cells (PC) and interneurons (IN).

	HL23PC	HL23IN	ML23PC	ML23IN
Soma volume	2384.02	2567.37	1522.12	220.68
Soma surface area	800.26	757.74	630.33	224.12
Soma radius	7.66	7.60	7.03	3.93
Max radial dist	837.61	518.19	401.93	383.39
Mean width	681.17	616.41	503.53	467.25
Mean height	1057.46	751.70	474.60	517.88
Mean depth	254.79	171.96	123.71	208.20

Table S3: Average morphometrics for neuronal reconstructions of layers 2 and 3 for mouse (M) and human (H) pyramidal cells (PC) and interneurons (IN).

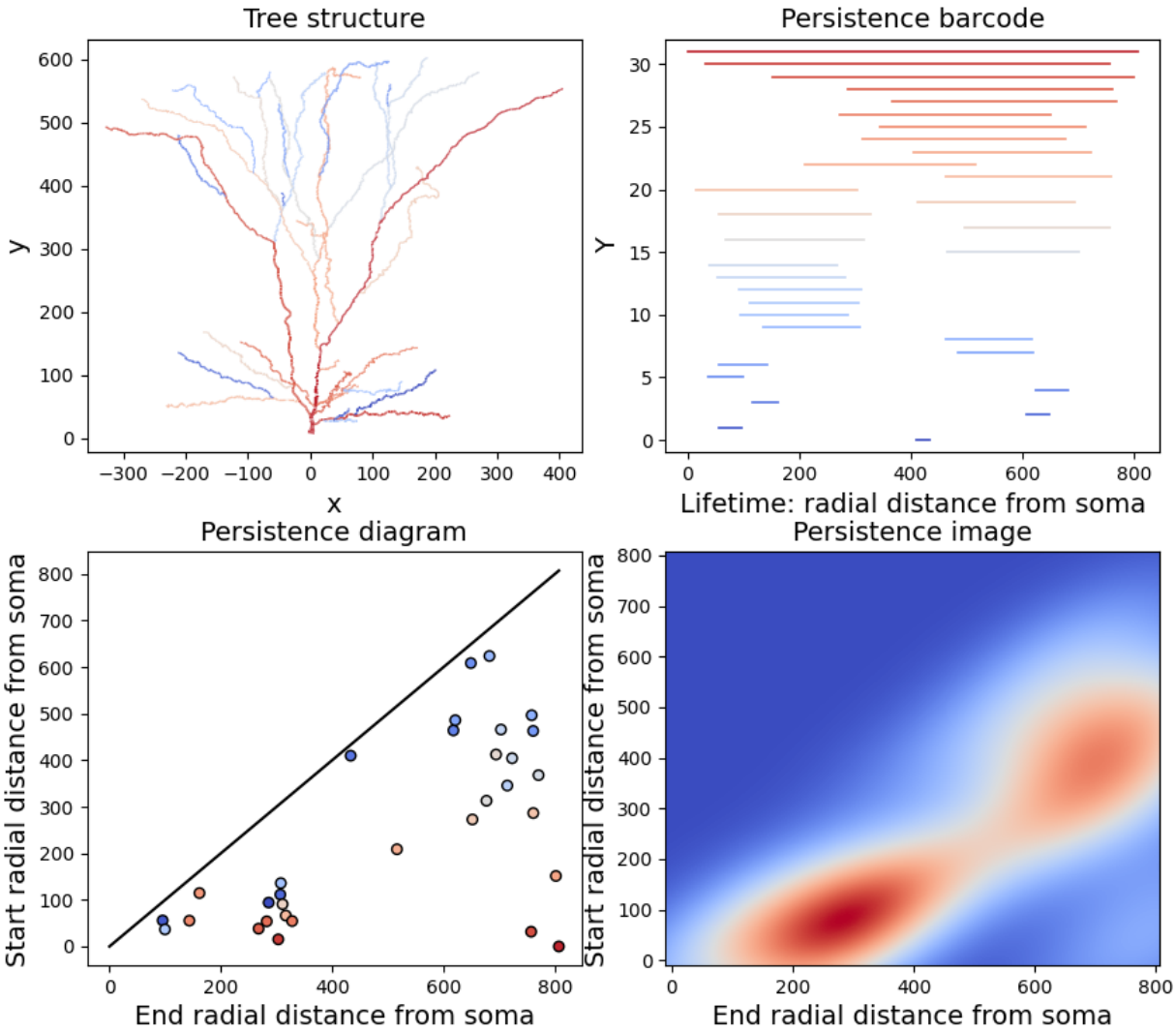

Figure 6: **Topological morphology descriptor of an exemplar human layer 2 - 3 pyramidal cell.** A. Apical dendrite, color-coded according to persistence components as illustrated in B. B. Persistence barcode, colormap from largest (red) to smallest branches (blue). C. Persistence diagram with the same color-code. D. Persistence image indicating areas of high density of branches (red) at different path distances from the soma (0,0).

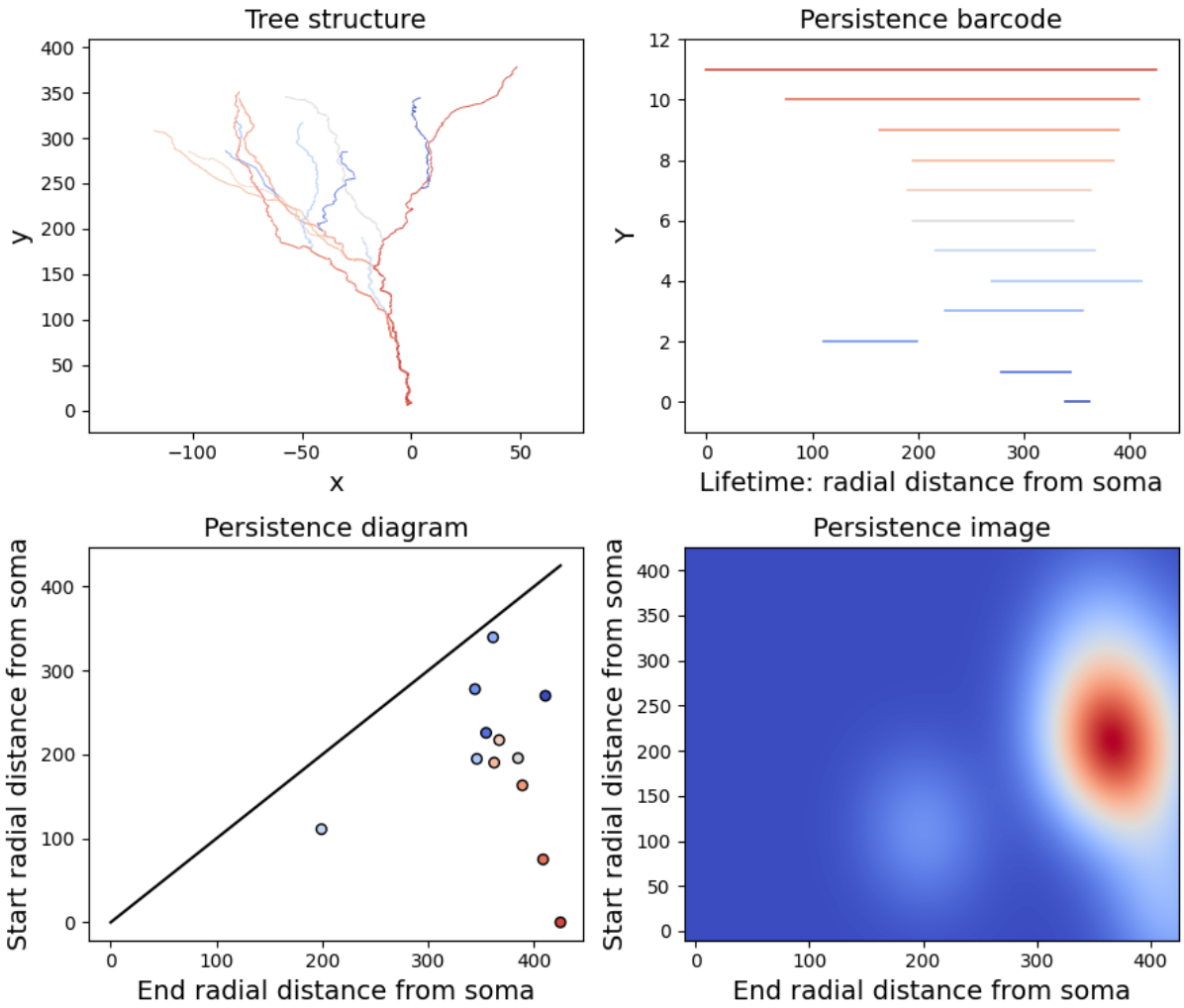

Figure 7: **Topological morphology descriptor of an exemplar mouse layer 2 - 3 pyramidal cell.** A. Apical dendrite, color-coded according to persistence components as illustrated in B. B. Persistence barcode, colormap from largest (red) to smallest branches (blue). C. Persistence diagram with the same color code. D. Persistence image indicating areas of high density of branches (red) at different path distances from the soma (0,0).

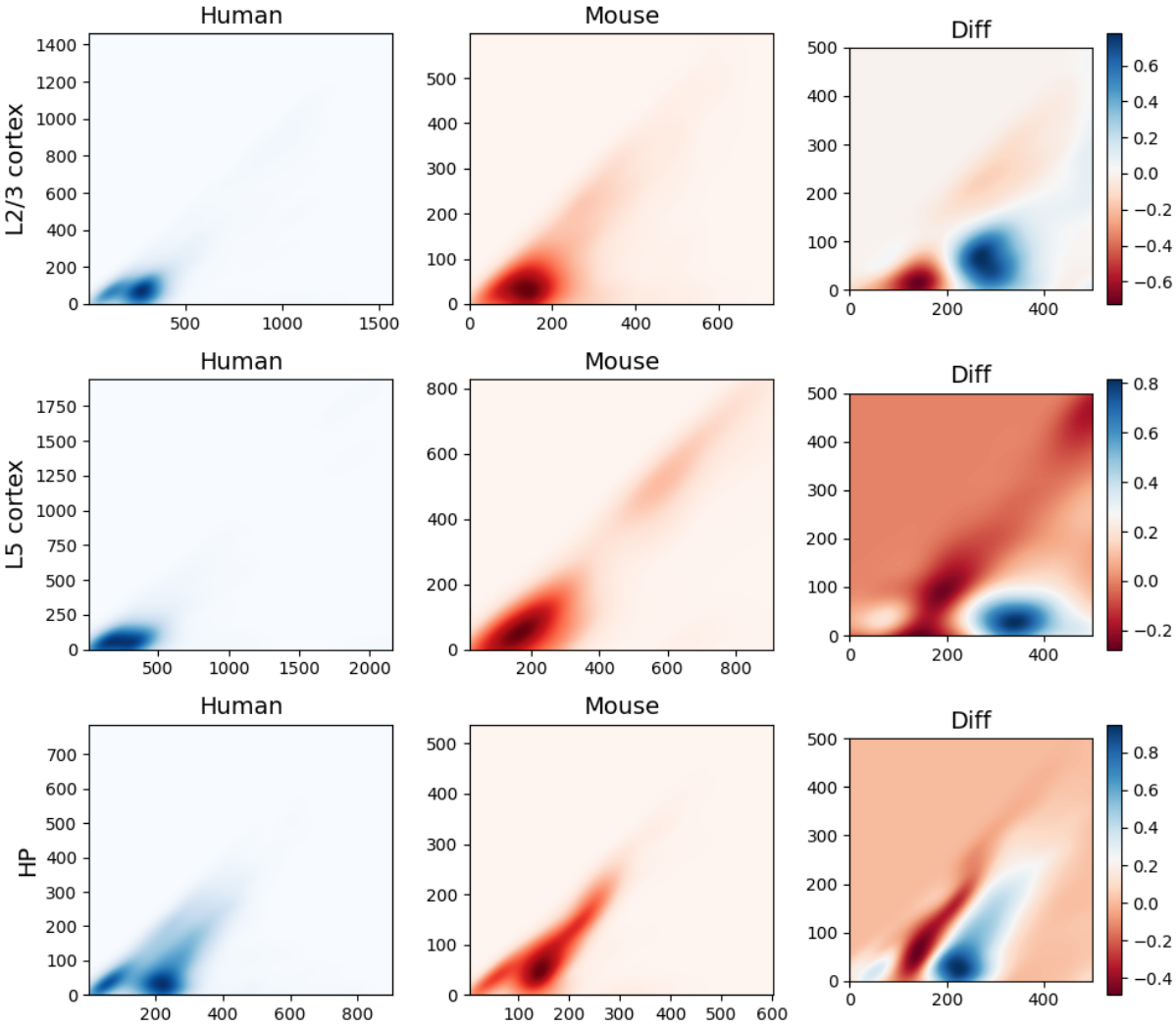

Figure 8: **Topological analysis of mouse and human pyramidal cells from cortical layers 2, 3, and 5 and hippocampus.** Column 1 shows the average persistence images for populations of human cells from different brain regions in blue. Column 2 shows the average persistence images for populations of mouse cells from different brain regions in red. Column 3 shows the average difference between the persistence images of human (blue) and mouse (red) cells from different brain regions. The topological differences that were observed between human and mouse pyramidal cells of layers 2 and 3 generalize to different layers and brain regions.

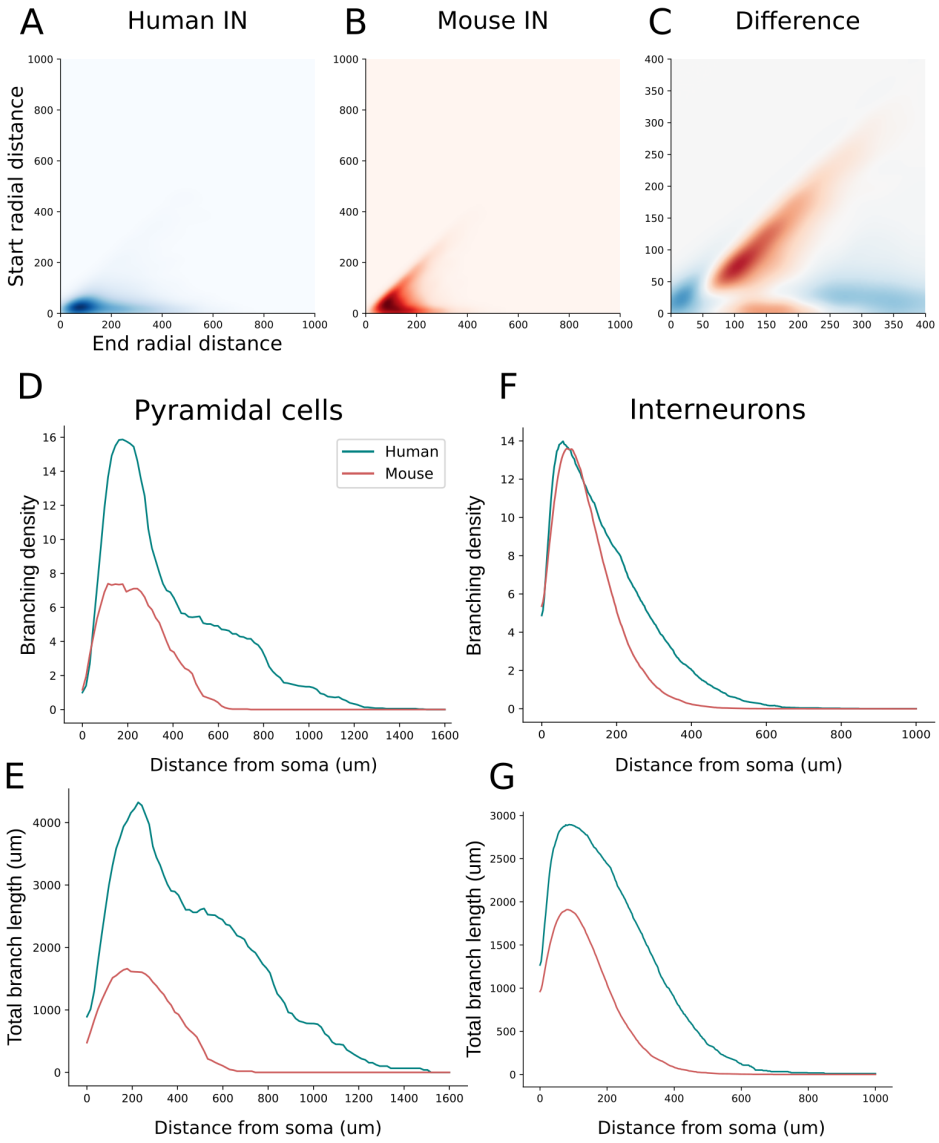

Figure 9: **Topological analysis of mouse and human interneurons from cortical layers 2 and 3.** A. Average persistence images for populations of human cells. B. Average persistence images for populations of mouse cells. C. shows the average difference between the persistence images of human (blue) and mouse (red) cells. The comparison of topological properties between pyramidal cells (D-E) and interneurons (F-G) of human (teal) and mouse (red) morphologies show that branching density is only marginally larger in interneurons (F), but branch lengths are significantly larger in human interneurons (G).

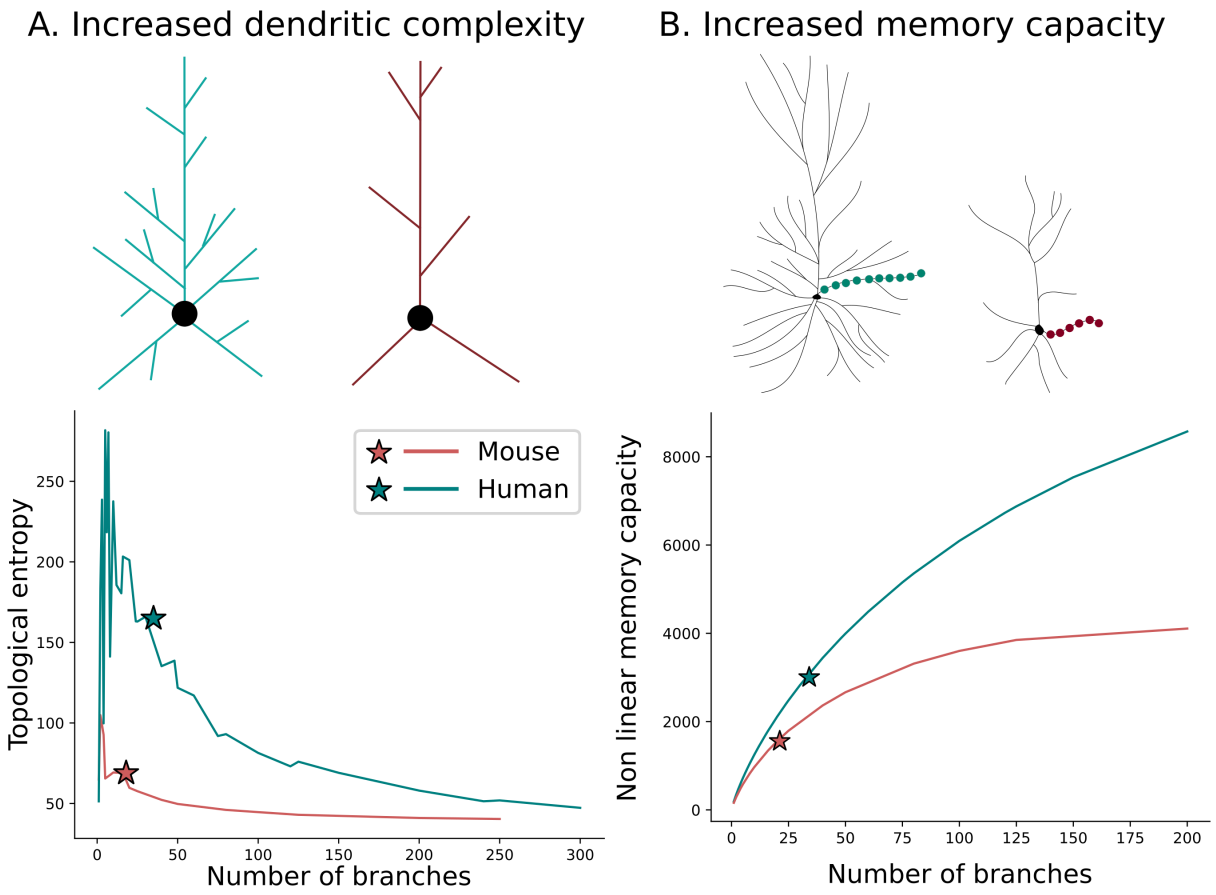

Figure 10: **Memory capacity is enhanced by cell complexity.** A. Cell complexity is measured by the topological entropy of the dendrites. Topological entropy is higher (almost twice) in human cells. B. Memory capacity is computed by the non-linear model in (Poirazi and Mel, 2001) and depends on the number of branches and their lengths. Memory capacity is higher (almost twice) in humans.